ρ = density
σ = growth rate for disturbance [Equation (14)]
σ_r, σ_i = real and imaginary parts, respectively, of growth rate
τ = tv/d^2 or, in Equation (19), = $(A1/a^4)^{1/3}$

Superscripts

— = stationary state solution
$\wedge$ = dimensional quantity

Subscripts

A = reactant A for the reaction $A \rightarrow m\,P$ with diffusion of products but no heat of reaction
d = evaluated at $z = d$ ($z = 1$)
P = product P for the reaction $A \rightarrow m\,P$ with diffusion of P but no heat of reaction
0 = evaluated at $z = 0$

LITERATURE CITED

1. Kenning, D. B. R., *Appl. Mech. Rev.*, **21**, 1101 (1968).
2. Pearson, J. R. A., *J. Fluid Mech.*, **4**, 489 (1958).
3. Sternling, C. V., and L. E. Scriven, *AIChE J.*, **5**, 514 (1959).
4. Nield, D. A., *J. Fluid Mech.*, **29**, 545 (1967).
5. Ruckenstein, E., and C. Berbente, *Chem. Eng. Sci.*, **19**, 329 (1964).
6. Chandrasekhar, S., "Hydrodynamic and Hydromagnetic Stability," Chap. I, II, Oxford Univ. Press, London (1961).
7. Wankat, P. C., and W. R. Schowalter, manuscript in preparation.
8. Mihaljan, J. M., *Astrophys. J.*, **136**, 1126 (1962).
9. Wankat, P. C., Ph.D. thesis, Princeton Univ. (1970).

Manuscript received November 12, 1970; revision received March 11, 1971; paper accepted March 12, 1971.

Application of Empirical Rate Expressions and Conservation Equations to Photoreactor Design

FRANCIS P. RAGONESE and JOHN A. WILLIAMS

Department of Chemical Engineering, Northeastern University, Boston, Massachusetts 02115

An empirical rate expression was obtained for the photolysis of tetrachloroplatinic acid (TCPA). The data used to evaluate the parameters of the rate expression were obtained in an elliptical photoreactor operated at high recycle rates in order to maintain a uniform reactant concentration within the photoreactor. A low-pressure mercury lamp provided light at a wavelength of 2,537Å. The light was assumed to enter the reactor radially and uniformly with respect to both the axial and angular directions.

This rate expression was incorporated in a reactant conservation equation which was solved to obtain the predicted conversion of TCPA in an elliptical photoreactor operating in the laminar regime. Solutions of the conservation equation were obtained for photoreactors of two different diameters and for three different lengths.

Experimentally observed conversions of TCPA in the laminar regime agreed well with the theoretical solutions except at conversions above 55%, where a solid precipitate apparently caused the lack of agreement.

The rational design and scale-up of photoreactors has been a subject of increasing interest to chemical engineers in recent years. The literature in this field has been critically reviewed by Cassano, Silveston, and Smith (5). The specific problem of photoreactor scale-up has been considered by Harris and Dranoff (9), who presented experimental results relating to the radial scale-up of an annular photoreactor, and by Dolan, Dimon, and Dranoff (7), who reported on the results of a dimensional analysis of an elliptical reflector-tubular photoreactor system. The tetrachloroplatinic acid photolysis reaction was utilized in both studies.

The scale-up methods developed by these authors do not require an explicit reaction rate expression. The method of Harris and Dranoff (9) is restricted to radial scale-up of annular photoreactors whose contents are well mixed.

The method of dimensional analysis was used by Dolan, Dimon, and Dranoff (7) to correlate conversion data obtained in a tubular flow photoreactor for a range of flow rates and length-to-diameter ratios. Since the correlation utilizes optical density as a parameter, this method cannot be used to predict photoreactor performance under conditions of varying optical density unless experimental data are available for every optical density encountered in the scale-up problem.

The purpose of the present work is to demonstrate an alternate approach to the problem of photoreactor scale-up. In this approach an empirical reaction rate expression, reactant continuity equation, and radiation equation are applied to the problem of predicting the performance of

F. P. Ragonese is with Shell Chemical Company, Woodbury, New Jersey 08096. Correspondence concerning this article should be addressed to J. A. Williams.

a tubular flow photoreactor under conditions of changing reactor dimensions and optical density. The photolysis of tetrachloroplatinic acid was observed experimentally in an elliptical reflector-tubular photoreactor in order to verify theoretical predictions of the photoreactor performance.

REACTION SYSTEM

The reaction selected for this investigation was the liquid phase photohydrolysis of tetrachloroplatinic acid in dilute aqueous solution. This reaction is promoted by ultraviolet light over a wide range of wavelengths at room temperature. Boll (2, 3) deduced that in the presence of ultraviolet light 10^{-4}M hexachloroplatinic acid will decompose as shown in Equations (1) and (2).

$$2\,H_2PtCl_6 + 11\,H_2O \xrightarrow{UV} 11\,HCl + H_2PtCl(OH)_5 \cdot H_2Pt(OH)_6 \quad (1)$$

$$H_2PtCl(OH)_5 \cdot H_2Pt(OH)_6 + H_2O \xrightarrow{UV} HCl + 2H_2Pt(OH)_{6\downarrow} \quad (2)$$

There probably are several intermediate steps in this reaction resulting in a stagewise elimination of chlorine from the original reactant to produce a chlorine-free precipitate of platinum hydroxide. Boll (2, 3) also studied the kinetics of this reaction and concluded that the reaction rate was a strong function of both reactant concentration and wavelength of the incident light but was relatively insensitive to temperature. It was not possible to deduce a reaction mechanism because intermediates could not be identified.

The photohydrolysis reaction results in the liberation of hydrochloric acid and in a change in the electrical conductivity of the solution. Dranoff and co-workers (7, 9) have utilized this phenomenon to follow the extent of the reaction by monitoring the change in electrical conductivity during the course of the reaction. In addition, they observed that freshly prepared solutions of hexachloroplatinic acid undergo a dark reaction which results in a slow increase in solution conductivity. They reported that after several days the conductivity of a 10^{-4}M solution of the acid levels off at a value corresponding to the conductivity of 2×10^{-4}M hydrochloric acid (8.5×10^{-5} mhos.). The same dark reaction and corresponding conductivity change were observed in the present study. It was concluded that hexachloroplatinic acid undergoes an initial dark reaction followed by two photochemical reactions as shown in Equations (3), (4), and (5).

$$H_2PtCl_6 + 2\,H_2O \xrightarrow{Dark} 2\,HCl + H_2Pt(OH)_2Cl_4 \quad (3)$$

$$2\,H_2Pt(OH)_2Cl_4 + 7\,H_2O \xrightarrow{UV} 7\,HCl + H_2PtCl(OH)_5 \cdot H_2Pt(OH)_6 \quad (4)$$

$$H_2PtCl(OH)_5 \cdot H_2Pt(OH)_6 + H_2O \xrightarrow{UV} HCl + 2\,H_2Pt(OH)_{6\downarrow} \quad (5)$$

Boll (2, 3) reported that solutions of tetrachloroplatinic acid follow the Beer-Lambert law. This was confirmed for acid solutions that were stabilized in the dark. The extent of the reaction was followed by monitoring solution transmission at a wavelength of 2,537Å. In general, the transmission readings were much more reproducible than electrical conductivity measurements.

Preliminary tests with a feed solution of 10^{-4}M tetrachloroplatinic acid resulted in severe wall deposits for conversions in excess of 30%. This yellowish-brown deposit, which lowered the transmission of the quartz reactor tube and had to be removed mechanically, was probably the platinum hydroxide formed according to Equation (5). Experiments conducted at concentrations of 0.4×10^{-4}M acid solution resulted in negligible wall deposits up to about 55% conversion. Therefore all experiments were conducted at a feed concentration of approximately 0.4×10^{-4}M.

EMPIRICAL RATE MODEL

In general the rate of a photochemical reaction is directly proportional to the volumetric rate of light absorption I_a raised to some power m. A general form for the reaction rate model of the single reactant A is given by Equation (6).

$$\Omega_A = kI_a^m\,\lambda(C_A) \quad (6)$$

This model indicates that the reaction rate is dependent upon some function of reactant concentration $\lambda(C_A)$. The rate constant k may be a function of both the wavelength of the absorbed radiation and the temperature of the fluid. When wall reactions occur, additional kinetic parameters must be introduced to account for this effect.

It was assumed that the tetrachloroplatinic acid photolysis reaction is of the nonchain, complex type and consequently the parameter $m = 1$. Since the function $\lambda(C_A)$ was not known for this reaction, it was assumed that it could be represented by C_A^n, where n is a constant to be determined. The method used to determine k and n was to perform a least-squares fit of the empirical rate model

$$\Omega_A = kI_aC_A^n \quad (7)$$

to rate data obtained from the photoreactor when operated at a high recycle ratio to approximate a continuous stirred-tank reactor (CSTR). The results of this analysis are discussed in a later section. The coupling of the empirical rate expression to the reactant continuity equation and radiation equation is considered below.

CONTINUITY AND RADIATION EQUATIONS

The reaction occurred in a tubular flow reactor, which is shown schematically in Figure 1. The intensity of the exciting radiation was assumed to be uniform and radially incident at the reactor surface. This model of light distribution has been assumed in experimental studies (6, 11)

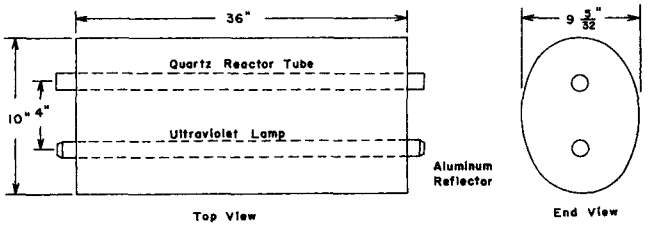

Fig. 1. Schematic diagram of elliptical reflector-photoreactor.

in which the reactor and lamp were aligned along the foci of an elliptical reflector.

The steady state continuity equation for the reactant A was expressed by Equation (8)

$$-v_z\frac{\partial C_A}{\partial z}+D_A\left[\frac{1}{r}\frac{\partial}{\partial r}\left(r\frac{\partial C_A}{\partial r}\right)\right]-\Omega_A=0 \quad (8)$$

in which the axial diffusion of reactant was assumed negligible. The reaction rate Ω_A is given by Equation (7).

The radiation equation for radial, monochromatic radiation in the case of the tubular flow reactor has been given by Harano and Smith (8) as

$$I(r,z)=\frac{2I_0R}{r}\left[\exp\left(-\alpha_A\int_0^R C_A(r',z)dr'\right)\right]\cdot\cosh\left[\alpha_A\int_0^r C_A(r',z)dr'\right] \quad (9)$$

Two special cases of Equations (8) and (9) were considered. Both cases involved the flow of a Newtonian fluid in the laminar regime.

Case 1. No radial diffusion: Equations (8) and (9) were written in dimensionless form by expressing the reactant concentration in terms of the fractional conversion, that is, $C_A = C_{A0}(1 - x_A)$, and by introducing the dimensionless parameters of optical density σ and reactor group Ψ where

$$\sigma \equiv \alpha_A\, C_{A0}\, D$$

$$\Psi \equiv \frac{k\, N_0}{Q\, C_{A0}^{1-n}}$$

The spatial variables r and z were written in dimensionless form using the transformations given in Equations (10) and (11):

$$\rho = r/R \quad (10)$$

$$\xi = z/L \quad (11)$$

When $D_A = 0$ the dimensionless form of the combined continuity equation and radiation equation is

$$\frac{\partial x_A}{\partial \xi}=\frac{\psi\sigma}{4}\frac{(1-x_A)^{n+1}}{\rho-\rho^3}\exp\left[-\frac{\sigma}{2}\int_0^1(1-x_A)d\rho\right]\cdot\cosh\left[\frac{\sigma}{2}\int_0^\rho(1-x_A)d\rho'\right] \quad (12)$$

The boundary condition for Equation (12) is

$$x_A(\rho,0)=0,\quad \xi=0 \quad (13)$$

The flow-averaged conversion at $\xi = 1$ is given by X_A where

$$X_A = 4\int_0^1(\rho-\rho^3)x_A(\rho,1)d\rho \quad (14)$$

Case II. Infinite Radial Diffusion: The integrated form of the combined continuity equation and radiation equation when $D_A = \infty$ is given in dimensionless form by

$$\psi=\int_0^{X_A}\frac{dX_A'}{(1-X_A')^n\{1-\exp[-\sigma(1-X_A')]\}} \quad (15)$$

The solutions to the above cases are conveniently presented in the form of a plot of fractional conversion X_A versus the reactor group Ψ. The performance of any real system operating in the laminar regime where the radial diffusivity is finite but not 0 is bounded by these solutions.

When the tubular flow reactor is operated at sufficiently large recycle ratios, its performance approximates that of a CSTR. The relation between ψ and X_A in this case is given by

$$\psi=\frac{X_A}{(1-X_A)^n\{1-\exp[-\sigma(1-X_A)]\}} \quad (16)$$

Equation (16) was used to predict the scale-up performance of the tubular flow photoreactor operating at large recycle ratios. This method of predicting reactor performance was tested experimentally, using the equipment and procedures described below.

EQUIPMENT

The arrangement of equipment is shown schematically in Figure 2. The apparatus consisted essentially of a reactor zone and a recycle system with provisions for feed introduction and product removal.

The reactor zone contained a cylindrical quartz reactor tube, an ultraviolet lamp, and an aluminum reflector. Two different 4-ft. reactor tubes with I.D. of 13 and 20 mm. were used. Ultraviolet radiation was supplied by a General Electric G36T6, 36-w., low-pressure, mercury germicidal lamp. Over 90% of the output of this lamp was at a wavelength of 2,537Å. This lamp was 36 in. long and ½ in. wide. An aluminum reflector with a length of 36 in. and an elliptical cross section of 9-5/32 in. × 10 in. was used to direct the radiation onto the reactor tube. This was accomplished by placing the lamp along one focus and the quartz reactor tube at the other focus of the elliptical cross section. For the elliptical cross section employed, the foci spacing was 4 in. The inside of the reflector was Alzak treated to provide a brightly reflecting surface. The reflector was fabricated by rolling 22-gauge (0.025 in. thickness) aluminum lighting sheet Alzak treated on one side into the desired elliptical cross section. The reflector was then mounted inside a plywood rib frame to maintain its shape.

Fresh reactant was pumped from a 6½ gal. darkened polyethylene feed tank into the reactor by a variable-speed tubing pump having a capacity of 1600 cu. cm./min. Interchangeable rotameters having ranges of 80 to 1600 cu. cm./min. were used to meter the flow rates of feed and product streams. For the CSTR operation the fluid in the reactor was recycled by a variable-speed, centrifugal pump having a capacity of 10 gal./min. The recycle stream flow rate was measured by a 0 to 10 gal./min. rotameter. In order to avoid cavitation at the recycle pump inlet, a liquid-level surge tube was located as shown in Figure 2. Two ¾ in. Flexiplug PVC valves were used to control the liquid level and to adjust the product flow rate. A cooling coil was installed inside the liquid-level surge tube in order to remove the heat produced by the recycle pump.

The recycle line was constructed from ¾ in. PVC pipe. All other materials of construction were selected on the basis of low metallic contamination. The quartz reactor tube was joined to the PVC recycle line by black rubber tubing and was sealed with silicone rubber cement. The only metallic parts in

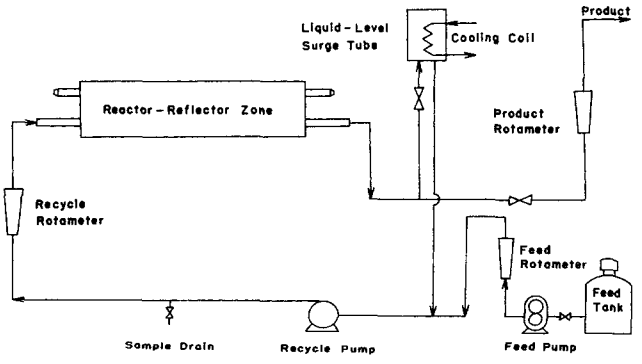

Fig. 2. Schematic diagram of experimental equipment.

contact with the reacting fluid were the stainless steel rotameter floats and a stainless steel pump impeller.

All transparent sections of the reactor system were shielded with black electrical tape or aluminum foil to eliminate any stray irradiation from the overhead laboratory lights. In addition, the ends of the reflector assembly were blocked off with opaque cardboard sheet.

PROCEDURE

Two different modes of reactor operation were employed in obtaining the experimental data. The procedures utilized for the continuous recycle mode and the tubular flow mode are discussed in this section. In each case the feed solution was approximately 0.4×10^{-4}M in tetrachloroplatinic acid. This solution was prepared in 20-liter batches by accurate dilution of a 0.01 M stock solution which had been aged in the dark for at least five days. All solutions were prepared with deionized-distilled water.

Recycle (CSTR) Operation

The kinetic measurements and scale-up tests of CSTR operation were conducted by operating the photoreactor in the recycle flow mode. At recycle rates equal to or greater than about 20 times the fresh feed rate, the recycle reactor behaves as a CSTR.

Prior to the start of a run, the lamp was turned on and allowed to warm up for at least 30 min. Stable lamp operation was indicated by constant readings of volt and amp meters connected in the lamp circuit.

The reactor was filled by charging approximately 2,500 cu. cm. of reactant through the open top of the liquid-level surge tube. Calibration marks on the liquid-level tube were used to directly indicate the exact volume of fluid in the reactor at any time. During the charging operation the product valve was kept closed, and the liquid-level valve was fully opened. After the reactant was added, the recycle pump was turned on, and the speed controller was set to give a recycle flow rate of at least 5 gal./min. Air removal was facilitated by purging small amounts of liquid reactant through drain and sample taps located at various points in the recycle line. The fluid was recirculated until all air bubbles were removed, at which time the feed pump was turned on and set at the desired flow rate. The product valve was then opened and adjusted to give a product flow rate equal to the feed flow rate. This adjustment was facilitated by using the same setting on both of the matched feed and product rotameters. Finally, the liquid level in the surge tube was regulated with the product and recycle valves to give a reactor volume of 2,500 cu. cm. At this time an electric timer was started to record the duration of the run.

Samples of the product stream were collected in 1.0-cm. spectrophotometer curvettes at approximately two-min. intervals. The percent transmission of each sample was recorded at a wavelength of 2,537°A. using a Hitachi Perkin-Elmer, Model 139, spectrophotometer. In addition to the product transmission readings, the feed and product temperatures, the product flow rate, and the recycle flow rate were recorded during each run. Although the feed and product rotameters were quite accurate, the product flow rate was measured during each run by determining the volume of fluid collected in a graduated cylinder over a given time period. Steady state conditions were attained when no further change in product transmission with time was observed. The time required to reach a steady state varied from about 10 to 40 min. for feed rates in the range of 1,000 to 100 cu.cm./min., respectively. After a steady state had been reached, the feed and product flow rates were changed to new values and another run was started. At the beginning and end of each run, the transmission of the feed material and the lamp voltage, amperage, and hours of operation were recorded. The reactor tube was checked for wall deposits after each series of runs made with a particular feed batch. By carrying out the first experimental runs at high flow rates and low conversions and then gradually increasing conversion, it was possible to eliminate the possibility of an early-run wall deposit ruining an entire series of runs.

Several series of CSTR runs were made at reactor diameters of 13 and 20 mm. with reactor lengths of 25 and 40 cm. Feed flow rates of these tests ranged from 138 to 1,190 cu. cm./min. The reactor length was changed without removing the quartz reactor tube by means of two sliding sections of black rubber tubing placed over the quartz tube at each end. These two 8-in. lengths of rubber tubing could be moved in either direction so that reactor lengths of 10 to 40 cm. were possible. Calibration markings at each end of the tube indicated the correct positions of the rubber guides for a given irradiation length. The only part of the quartz tube exposed to radiation was the section between the rubber guides. This rapid and simple method of changing reactor lengths eliminated the need for removal of the reactor tube and thus decreased the number of actinometer measurements necessary for a given reactor diameter.

Tubular Flow Operation Mode

For these experiments the reactor system was modified by disconnecting the recycle line, the liquid-level surge tube, and the product rotameter. Feed was pumped through the feed rotameter and directly into the quartz reactor tube. No particular cooling requirements were necessary for this operation mode since the temperature rise resulting from the ultraviolet lamp was negligible. Product transmission, feed temperature, product temperature, feed transmission and feed flow rate were measured periodically, as in the CSTR procedure, until a steady state was achieved. Usually only 5 to 10 min. was required to reach a steady state.

Several series of tubular flow runs were made at reactor diameters of 13 and 20 mm. with reactor lengths of 15, 25, and 40 cm. and feed flow rates of 97 to 1,320 cu. cm./min.

EXPERIMENTAL KINETIC RESULTS

The experimental data for the kinetic analysis are discussed according to the following categories: (1) the actinometer data used to determine the energy input to the reactor, (2) the spectrophotometer data used to test the validity of the Beer-Lambert law as applied to solutions of tetrachloroplatinic acid and water, and (3) CSTR operation data using the tetrachloroplatinic acid system.

Actinometer Studies

The results of the potassium ferrioxalate actinometer tests are shown in Table 1. The details of the actinometer procedure are presented in the Appendix. Runs were made at reactor lengths of 15, 30, 40, and 50 cm. for the

Table 1. Lamp Calibration Data Using the Potassium Ferrioxalate Actinometer

Reactor diameter, cm.	1.3	1.3	1.3	1.3	2.0
Reactor length, cm.	15	30	40	50	40
Feed rate, liters/min.	0.208	0.210	0.211	0.210	0.353
Feed temperature, °F.	78.0	78.0	78.0	78.0	80.5
Product temperature, °F.	78.0	78.0	78.0	78.0	80.5
Product sample volume, cu. cm.	1.0	1.0	1.0	1.0	1.0
Dilute sample volume, cu. cm.	25.0	25.0	25.0	25.0	25.0
% transmission of diluted sample at 510 mμ	57.7	33.0	22.0	15.0	35.2
Concentration of Fe^{+2} in product, g.-mole/liter $\times 10^4$	5.37	10.83	14.40	18.40	10.20
Incident power einsteins/min. $\times 10^4$	0.92	1.88	2.51	3.20	2.98
Incident intensity einsteins/(min.)(cm.) $\times 10^6$	1.51	1.54	1.54	1.57	1.19

Table 2. UV Transmission Data for Standard Solutions of Tetrachloroplatinic Acid and Water

Concentration of $H_2PtCl_4(OH_2)$, g.-mole/liter $\times 10^4$	% Transmission 1.0-cm. cell 253.7 mμ
1.000	3.0
0.800	6.0
0.600	12.2
0.400	24.7
0.200	49.8
0.120	65.7
0.040	87.0

1.3-cm. diam. tube and at 40 cm. for the 2.0-cm. diam. tube. In each case the incident power (in einsteins per minute) was found to be in direct proportion to reactor length. This result indicates uniform irradiation of the reactor tube in the axial direction.

As the reactor diameter was increased from 1.3 to 2.0 cm. at a reactor length of 40 cm., the intensity of radiation incident on the reactor surface decreased from 1.54 $\times$ 10^{-6} to 1.19 $\times$ 10^{-6} einsteins/(sq.cm.)(min.). This finding is of significance and will be discussed in a following section.

Reactant Solution Optics

Several solutions of tetrachloroplatinic acid and water having concentrations of 0.04, 0.12, 0.20, 0.40, 0.60, 0.80, and 1.00 $\times$ 10^{-4}M were prepared from a standard 0.10M solution of the acid. The percent transmission of each of these samples was recorded at a wavelength of 2,537Å. The results of these measurements are shown in Table 2. It is quite clear from these data that even very dilute solutions of this acid strongly absorb ultraviolet energy at a wavelength of 2,537Å. In particular, solutions of this acid having concentrations greater than about 0.30 $\times$ 10^{-4}M may be considered as strong absorbers since more than half of the incident energy is absorbed in a 1.0-cm. layer of the solution.

The Beer-Lambert law of solution optics was used in the mathematical models to describe the attenuation of incident light with position in the reactor tube. A semilog plot of the reactant concentration versus solution transmission in percent yielded a straight line, the slope of which corresponds to the extinction coefficient α_A. The slope was 3.5 $\times$ 10^{-4} liter/(g.-mole)(cm.).

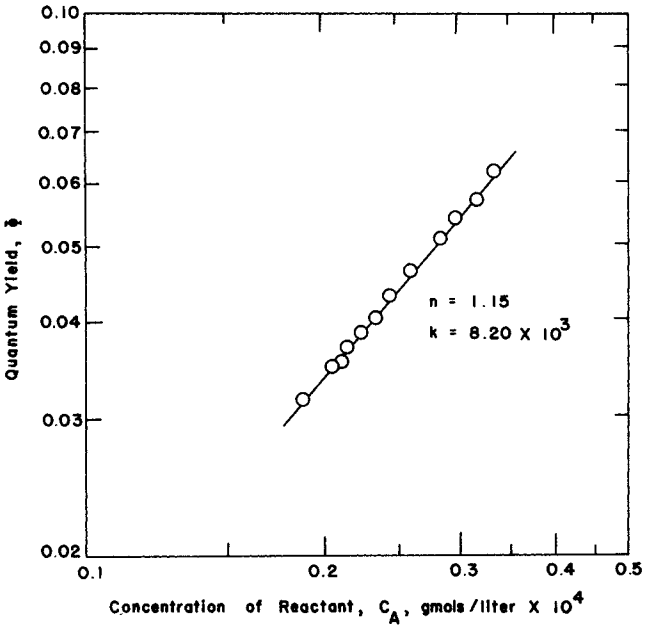

Fig. 3. Least-squares fit of experimental kinetic data.

CSTR Operation

The results of the CSTR kinetic tests are presented in Table 3. All of these runs were made with a feed concentration of approximately 0.4 $\times$ 10^{-4}M tetrachloroplatinic acid. As feed flow rate was varied from 0.138 to 1.190 liters/min., the steady state product concentrations ranged from 0.190 $\times$ 10^{-4} to 0.339 $\times$ 10^{-4}M. Under these conditions reactant conversions of 16.3 to 53.2% and quantum yields of 0.0318 to 0.0621 were obtained with a 25-cm. irradiation length and a 1.3-cm. diam. tube. The volumetric rate of energy absorption and reaction rates reported in Table 3 are based on the total irradiated volume plus the recycle reactor volume of 2.5 liters.

A log-log plot of quantum yield versus reactant concentration should yield a straight line whose slope corresponds to the reaction order according to Equation (7). In Figure 3 the least-squares line is shown along with the experimental data points. The reaction rate constant k is 8.20 $\times$ 10^3 and the reaction order n is 1.15. A comparison of calculated reaction rates, using the above kinetic parameters, with experimental reaction rates indicates deviations ranging from 0.04 to 0.79% with an average deviation of $\pm$ 0.38%. These results imply that the reaction system is

Table 3. Experimental Results for CSTR Kinetic Analysis

Run no.	Product conc. $\times 10^4$ g.-moles/liter	Absorbed power $\times 10^5$ einstein/(liter)(min.)	Quantum yield	Reaction rate $\times 10^6$ g.-moles/(liter)(min.) Exp.	Calc.	% Deviation of calculated from experimental
1A	0.339	5.06	0.0621	3.142	3.126	0.49
2A	0.320	4.94	0.0574	2.832	2.854	0.79
3A	0.302	4.81	0.0540	2.596	2.602	0.24
4A	0.288	4.70	0.0512	2.410	2.409	0.04
5A	0.263	4.49	0.0465	2.090	2.074	0.76
6A	0.247	4.35	0.0430	1.871	1.867	0.18
7A	0.235	4.23	0.0405	1.714	1.716	0.14
8A	0.225	4.13	0.0387	1.598	1.593	0.34
9A	0.217	4.04	0.0368	1.489	1.496	0.50
10A	0.212	3.99	0.0358	1.428	1.437	0.62
11A	0.208	3.94	0.0354	1.395	1.390	0.33
12A	0.190	3.73	0.0318	1.187	1.185	0.13

approximately first order with respect to the reactant concentration. It was not possible, however, to deduce a first-order reaction rate model from mechanistic considerations since lack of knowledge of the photohydrolysis intermediates precluded such an analysis. In any case, the reaction rate model obtained from the CSTR data accurately represents the reaction rate data over the concentration range investigated.

COMPARISON OF THEORY WITH EXPERIMENTS

The empirical rate model was coupled to the continuity and radiation equations which were integrated in order to predict the performance of the photoreactor operating under conditions of variable length and diameter. Comparisons of the predicted performance with experimental observations are given below.

Theoretical Results for Reaction System

Each of the three proposed mathematical models representing the photoreactor performance can be solved after specifying values of the reactor group ψ, reaction order n, and the optical density σ. Reactor diameters of 1.3 and 2.0 cm., employed experimentally in the various runs, correspond to optical densities of 1.89 and 2.90, respectively. These values of optical density are based on the initial reactant concentration of 0.415×10^{-4}M.

Theoretical results for the conversion-reactor group relationship are shown in Figures 4 and 5 for a reaction order of 1.15 and optical densities of 1.89 and 2.90. These figures show the theoretical relationships among the two laminar flow cases and the CSTR model.

CSTR Flow Case: Longitudinal and Radial Scale-Up

The results of the longitudinal scale-up test for CSTR operation are presented in Figure 4. These runs were conducted at a reactor length of 40 cm. and a reactor diameter of 1.3 cm. The deviations between the experimental and theoretical conversions range from 0 to 6.77% based on conversions of 31.0 to 50.5% and reactor groups of 0.73 to 1.99. The mean deviation was 5.40%. The results obtained for CSTR operation under conditions of simultaneous longitudinal and radial scale-up are shown

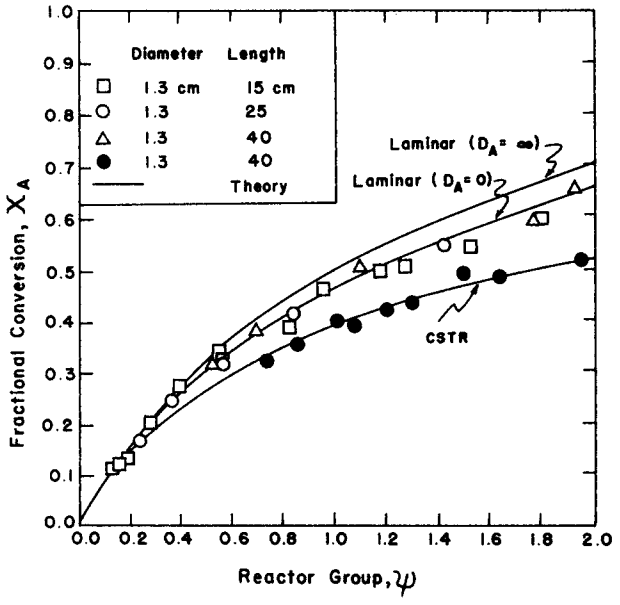

Fig. 4. Comparison of theory and experimental results for an optical density of 1.89.

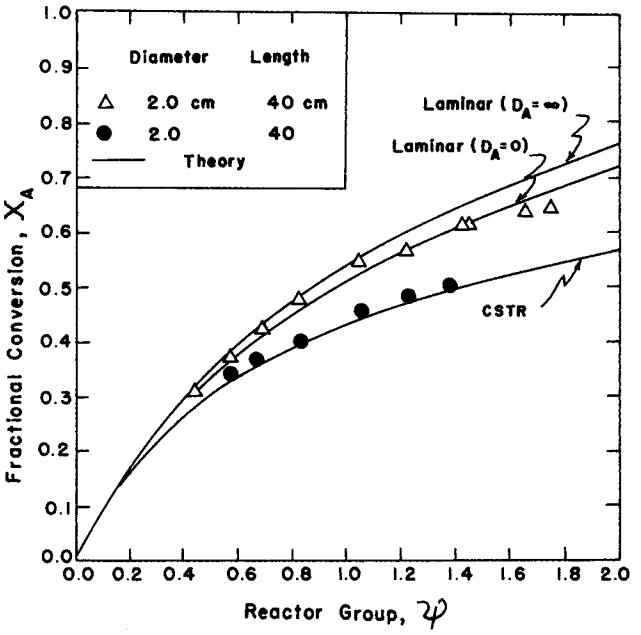

Fig. 5. Comparison of theory and experimental results for an optical density of 2.90.

in Figure 5. The experimental conversions are slightly greater than predicted by theory. The deviations range from 2.77 to 7.65% with a mean of 4.94%.

These results indicate that the CSTR flow model adequately predicts conversions for CSTR operation of the tubular flow photoreactors for the lengths and diameters used in this work.

Tubular Flow Case: Longitudinal and Radial Scale-Up

Experiments were conducted under tubular flow conditions (no recycle), where the Reynolds numbers ranged from 171 to 2,200.

The results of the longitudinal scale-up tests under laminar flow conditions are compared with the theoretical laminar flow models in Figure 4. The longitudinal scale-up runs were accomplished at an optical density of 1.89 with reactor lengths of 15, 25, and 40 cm. The comparison of experimental conversions with the laminar flow model when $D_A = \infty$ resulted in deviations of 0.74 to 17.89% for conversions of 11.2 to 65.0% and reactor groups of 0.14 to 1.92. Over the same range of conversions, the laminar flow model with $D_A = 0$ gave deviations of 0 to 10.53%.

The laminar flow tests conducted at an optical density of 2.90 and a reactor length of 40 cm. represent conditions of simultaneous longitudinal and radial scale-up. These results, shown in Figure 5, are bounded by the solutions of the two laminar flow models except at the largest conversions observed.

Most of the larger differences between the theoretical and experimental results occur for those cases in which the conversion exceeded 55%. Under these conditions the yellow precipitate mentioned earlier tends to coat the reactor wall and reduce the incident light intensity. This reduced incident intensity is believed responsible for the lower conversions in this operating region.

The mean deviation for the laminar flow models for all of the tubular flow tests is 5.65%. These results indicate that the laminar flow model adequately predicts the performance of the tubular flow photoreactor operating in the laminar regime.

DISCUSSION

The assumptions made in this work are discussed in relation to their effect on the results obtained. A principal assumption was that the formation of wall deposits and suspended solid precipitates was avoided at low conversions. If wall deposits were formed they would reduce the amount of radiant energy received by the reacting solution and thus lead to lower experimental conversions than predicted from theory. Furthermore, due to the scattering effect of suspended solids, the reactant analysis would indicate less conversion than actually occurred. Since this type of disagreement between theory and experiment was observed only at larger conversions, it is likely that precipitate formation was avoided at lower conversions.

It was assumed that the radiant energy was radially incident at the reactor walls and uniformly distributed both angularly and axially. The actinometer measurements reported establish that the light is axially uniform. The assumption of angular uniformity cannot be established from the actinometer measurements. The actinometer measurements for reactors of different diameter indicate that the light is not entirely radially incident. If the light were radially incident, then the rate of energy input to reactors of different radii but of the same length should be identical. This relationship, expressed by Equation (17), depends upon locating each tube concentric with the reflector focus and may not be attainable in practice.

$$(I_0 \cdot R)_1 = (I_0 \cdot R)_2 \qquad (17)$$

In Equation (17) the subscripts 1 and 2 represent the smaller and larger tubes used in this work, respectively. The measurements previously reported show that the rate of energy input did not remain constant when the tube diameter was changed from 1.3 to 2.0 cm. From Equation (17) the ratio of wall energy fluxes should theoretically be

$$\frac{(I_0)_1}{(I_0)_2} = \frac{R_2}{R_1} = \frac{2.0}{1.3} = 1.54$$

while actually

$$\frac{(I_0)_1}{(I_0)_2} = 1.295$$

If the light was randomly oriented at the reactor surface then one would expect the rate of energy input to be directly proportional to the tube radius, In this case

$$\frac{(I_0)_1}{(I_0)_2} = 1 \qquad (18)$$

Although the assumption of radially incident light is not entirely correct, it appears to be a better assumption in this case than that of a diffuse light distribution model.

Finally, it should be noted that the experimental conversions shown in Figures 4 and 5 had to be compared to the conversions predicted from laminar flow models at extreme values of the reactant radial diffusivity coefficient since the actual value of D_A was unknown. Fortunately the difference in conversion between models is small in the optical density range encountered in this work. Hill, Reiss, and Shandalman (*10*) also reported a small difference in conversion for a zero-order reaction ($n = 0$) at extreme radial diffusion rates in a tubular flow photoreactor.

It is believed that the difference in conversion predicted by the models for the present reaction would increase under conditions of large optical density. In the limit as $\sigma \rightarrow \infty$ Williams and Ragonese (*12*) have shown that the conversion tends to 0 in the case of no radial diffusion and is given by

$$X_A = 1 - \exp(-\psi)$$

in the case of infinitely rapid radial diffusion. While this result was obtained for a first-order reaction ($n = 1$), it is reasonable to assume that the present reaction, where $n = 1.15$, would behave in a similar manner. These authors also showed that, in the case of no radial diffusion, incident light energy is utilized most efficiently by a first-order reaction in the optical density range of 6 to 8, depending on the conversion. Therefore it is expected that differences in conversion between models in the present case would increase with increasing values of optical density above the range of 6 to 8.

This work has demonstrated the successful application of an empirical rate expression to the problem of predicting photoreactor performance. Although the results obtained here cannot be generalized to apply to other photoreactions, the methods used are general. For any particular photoreaction the use of empirical rate expressions would be justified if all variables affecting the rate were considered in the model. If the reaction was not understood, then much preliminary experimentation would be required to obtain an adequate rate expression. Such efforts would have to be justified in terms of one's increased understanding of the reaction and abilities to rationally design a photoreactor in which the reaction is conducted.

NOTATION

C_A = concentration of the single reactant A or tetrachloroplatinic acid, g.-mole/liter
C_{A0} = initial concentration of reactant A, g.-mole/liter
C_A' = dummy concentration variable of integration
C_{Fe+2} = concentration of ferrous ion in actinometer leaving reactor, g.-mole/liter
d = spectrophotometer cell pathlength, cm.
D = reactor diameter, cm.
D_A = molecular diffusivity of species A, sq.cm./min.
$[Fe^{+2}]$ = ferrous ion concentration in diluted actinometer sample, g.-mole/liter
I = light intensity, einstein/(sq.cm.)(min.)
I_0 = incident light intensity, einstein/(sq.cm.)(min.)
I_a = volumetric rate of light absorption, einstein/(liter)(min.)
k = reaction rate constant, $(\text{liters})^n/(\text{einstein})(\text{g.-mole})^{n-1}$
L = reactor length, cm.
n = reaction order, dimensionless
N_0 = total incident energy, einstein/min.
Q = feed flow rate, liter/min.
r = radial position variable, cm.
r' = dummy radial variable of integration
R = reactor radius, cm.
t = time, min.
V = reactor volume, liter
V_1 = irradiated sample volume for actinometer analysis, cu.cm.
V_2 = volumetric flask volume for actinometer analysis, cu.cm.
v_z = axial velocity, cm./min.
$\bar{v}_z$ = average axial velocity, cm./min.
x_A = fractional conversion of reactant A, dimensionless
X_A = flow-averaged conversion, dimensionless
z = axial position variable, cm.

Greek Letters

α_A = absorption coefficient for single reactant A, liter/(g.-mole)(cm.)
α_f = absorption coefficient for ferrous ion, liter/(g.-mole)(cm.)
ξ = z/L, dimensionless axial position variable
ρ = r/R, dimensionless radius variable
ρ' = dummy dimensionless radial variable of integration
ψ = reactor group, dimensionless
Φ = quantum yield, g.-mole/einstein
Φ_f = quantum yield of actinometer system, g.-mole/einstein
σ = $\alpha_A C_A D$, optical density, dimensionless
Ω_A = reaction rate of reactant A, g.-mole/(liter)(min.)
$\Omega_{Fe} + 2V$ = production rate of ferrous ions, g.-mole/min.

Subscripts

A = single reactant or tetrachloroplatinic acid
0 = initial or incident condition

LITERATURE CITED

1. Baxendale, J. H., and N. K. Bridge, *J. Phys. Chem.*, **59**, 783 (1955).
2. Boll, M., *Ann. Phys. (Paris)*, **2**, 5 (1915).
3. *Ibid.*, 226 (1915).
4. Calvert, J. G., and J. N. Pitts, "Photochemistry," 1st edit., Wiley, New York (1966).
5. Cassano, A. E., P. L. Silverston, and J. M. Smith, *Ind. Eng. Chem.*, **59**, 18 (1967).
6. Cassano, A. E., and J. M. Smith, *AIChE J.*, **13**, 915 (1967).
7. Dolan, W. J., C. A. Dimon, and J. S. Dranoff, *ibid.*, **11**, 1000 (1965).
8. Harano, Y., and J. M. Smith, *ibid.*, **14**, 584 (1968).
9. Harris, P. R., and J. S. Dranoff, *ibid.*, **11**, 497 (1965).
10. Hill, R. B., N. Reiss, and L. H. Shendalman, *ibid.*, **14**, 798 (1968).
11. Huff, J. E., and C. A. Walker, *ibid.*, **8**, 193 (1962).
12. Williams, J. A., and F. P. Ragonese, *Chem. Eng. Sci.*, **25**, 1751 (1970).

Manuscript received January 10, 1971; revision received April 21, 1971; paper accepted April 22, 1971. Paper presented at AIChE Puerto Rico meeting.

APPENDIX

The quantitative determination of quantum yields in experimental photochemistry requires knowledge of the power input of the lamp source at the fluid-reactor wall interface. The rate of energy input N_0 must be known in order to evaluate the reaction quantum yield. The rate of energy input and the incident light intensity may be determined by applying the principles of chemical actinometry. A discussion of several common types of chemical actinometers has been presented by Calvert and Pitts (*4*). The potassium ferrioxalate reaction system is a sensitive actinometer. The procedures utilized in applying this actinometer to the present study are presented below.

Solution Preparation

Solutions of potassium ferrioxalate in sulfuric acid were prepared according to the procedure of Baxendale and Bridge (*1*). Each liter of solution contained the following: (1) 2.41 g. of ferric ammonium sulfate, $FeNH_4(SO_4)_2 \cdot 12\,H_2O$; (2) 2.49 g. of potassium oxalate, $K_2C_2O_4$; (3) 2.7 cu.cm. of concentrated (18 M) sulfuric acid, H_2SO_4.

The resulting solution prepared from distilled water was approximately 0.005M ferric ammonium sulfate, 0.015M potassium oxalate and 0.10N sulfuric acid. The actinometer solution was prepared and stored in a 6.5-gal., darkened, polyethylene tank. Within a few hours, the above mixture stabilizes into a solution which is approximately 0.005M potassium ferrioxalate.

Reactor Operating Procedure

The tubular flow (no recycle) operational mode was used for all of the actinometer runs. The ultraviolet lamp was allowed to warm up for at least 30 min. The feed pump was turned on, and the feed rate adjusted to give a flow of about 200 to 300 cu.cm./min. This flow condition was maintained for approximately 10 min. At this time several 50-cu.cm. samples of the effluent stream were taken at 2-min. intervals. During each run the feed temperature, product temperature, lamp amperage, lamp voltage, and product flow rate were measured.

Product Analysis

Ultraviolet light absorption by solutions of potassium ferrioxalate results in the formation of ferrous ions. The ferrous ion concentration in the reactor output stream was determined spectrophotometrically. This was accomplished by adding 1.0 cu.cm. of irradiated sample, 3.0 cu.cm. of 1.0M sodium acetate and 3.0 cu.cm. of 0.1% by weight of 1,10 phenanthroline indicator to a 25-cu.cm. volumetric flask. This mixture was diluted to 25 cu.cm. with distilled water and allowed to remain in the dark for 1 hr. A blank solution was prepared in a similar manner using an unirradiated sample. This solution was also aged for 1 hr. in the dark. The fractional transmission of each solution at 5,100Å. in a 1.0-cm. cell was measured using the blank solution in the reference beam of the spectrophotometer.

Incident Power Determination

The concentration of ferrous ion in the diluted sample was determined by utilizing the Beer-Lambert law in the following form:

$$\frac{I}{I_0} = 10^{-\alpha_f [Fe^{+2}] d} \tag{19}$$

For a 1.0-cm. cell, Equation (19) may be rewritten as

$$[Fe^{+2}] = \log_{10} [I_0/I]/\alpha_f \tag{20}$$

The concentration of ferrous ion in the reactor exit stream, $C_{Fe} + 2$, is calculated as follows:

$$C_{Fe} + 2 = V_2 [Fe^{+2}]/V_1 \tag{21}$$

The potassium ferrioxalate reaction is zero order in reactant concentration and first order in the absorbed radiation intensity. In addition, the absorption coefficient at a wavelength of 2,537Å. is very large for a 0.005M solution of potassium ferrioxalate (*4*). For this reason, the absorption of the incident energy in the flow reactor experiments was essentially complete. For a zero-order reaction at high optical density, the laminar flow and CSTR flow conversion characteristics are nearly identical for conversions less than about 50%. For this reason, a CSTR mass balance on product ferrous ions is applied to the actinometer flow tests as follows:

$$Q[C^0_{Fe} + 2 - C_{Fe} + 2] + \Omega_{Fe} + 2\,(V) = 0 \tag{22}$$

The production rate of ferrous ions may be expressed as

$$\Omega_{Fe} + 2\,(V) = \phi_f N_0 \tag{23}$$

The inlet reactor concentration $C^0_{Fe} + 2$ is zero since a blank prepared from the feed solution was used in the reference beam of the spectrophotometer. Under these conditions, Equations (22) and (23) are combined to give

$$N_0 = QC_{Fe} + 2/\phi_f \tag{24}$$

The quantum yield ϕ_f for this reaction is 1.21 at a wavelength of 2,537Å. (*1*). Equation (24) was used to calculate the power input N_0 from the actinometer data.